**Acta Pharmacologica Sinica** 2017: 1435–1444
 1671-4083/17
www.nature.com/aps

Original Article

# Pharmacokinetic and metabolomic analyses of the neuroprotective effects of salvianolic acid A in a rat ischemic stroke model

Si-qi FENG[1, #], Nan AA[2, #], Jian-liang GENG[1], Jing-qiu HUANG[1], Run-bin SUN[1], Chun GE[1], Zhi-jian YANG[2, *], Lian-sheng WANG[2], Ji-ye AA[1, *], Guang-ji WANG[1]

[1]*Key Laboratory of Drug Metabolism and Pharmacokinetics, State Key Laboratory of Natural Medicines, Jiangsu Key Laboratory of Drug Design and Optimization, China Pharmaceutical University, Nanjing 210009, China;* [2]*Department of Cardiology, The First Affiliated Hospital of Nanjing Medical University, Nanjing 210029, China*

**Abstract**

Salvianolic acid A (SAA), a water-soluble phenolic acid isolated from the root of Dan Shen, displays distinct antioxidant activity and effectiveness in protection against cerebral ischemia/reperfusion (I/R) damage. However, whether SAA can enter the central nervous system and exert its protective effects by directly targeting brain tissue remains unclear. In this study, we evaluated the cerebral protection of SAA in rats subjected to transient middle cerebral artery occlusion (tMCAO) followed by reperfusion. The rats were treated with SAA (5, 10 mg/kg, iv) when the reperfusion was performed. SAA administration significantly decreased cerebral infarct area and the brain water content, attenuated the neurological deficit and pathology, and enhanced the anti-inflammatory and antioxidant capacity in tMCAO rats. The concentration of SAA in the plasma and brain was detected using LC-MS/MS. A pharmacokinetic study revealed that the circulatory system exposure to SAA was equivalent in the sham controls and I/R rats, but the brain exposure to SAA was significantly higher in the I/R rats than in the sham controls (fold change of 9.17), suggesting that the enhanced exposure to SAA contributed to its cerebral protective effect. Using a GC/MS-based metabolomic platform, metabolites in the serum and brain tissue were extracted and profiled. According to the metabolomic pattern of the tissue data, SAA administration significantly modulated the I/R-caused perturbation of metabolism in the brain to a greater extent than that in the serum, demonstrating that SAA worked at the brain tissue level rather than the whole circulation system. In conclusion, a larger amount of SAA enters the central nervous system in ischemia/reperfusion rats to facilitate its protective and regulatory effects on the perturbed metabolism.

**Keywords:** salvianolic acid A; stroke; cerebral ischemia/reperfusion injury; pharmacokinetics; metabolomics

*Acta Pharmacologica Sinica* (2017) 38: 1435–1444; doi: 10.1038/aps.2017.114; published online 24 Aug 2017

## Introduction

Stroke is the second leading cause of morbidity and mortality throughout the world[1]. Ischemic stroke[2], which mainly results from cerebral artery occlusion, accounts for 80% of strokes. Thrombolysis is very common clinically because it quickly increases blood flow to the brain and greatly promotes neural function recovery[3, 4]. However, an instant supply of blood flow in reperfusion may cause severe damage to the nervous system, namely, ischemia/reperfusion injury. This process involves energy depletion, calcium overload, reactive oxygen species accumulation, the neurotoxic effect of excitatory amino acids, inflammation, apoptosis, *etc*[5-7]. In addition, the permeability of the blood brain barrier increases during cerebral ischemia/reperfusion injury[8].

*Salvia miltiorrhiza* (SM, also known as Dan Shen) is one of the most well-known traditional Chinese medicines. It has been used for centuries and applied clinically for the treatment of various diseases, including myocardial infarction, hyperlipidemia, and atherosclerosis[9-12]. Salvianolic acid A (SAA) is one of the main water-soluble phenolic acids isolated from the root of Dan Shen and shows the most potent antioxidative activity against peroxidative damage (Figure 1)[13, 14]. SAA has been well-documented to possess a variety of significant pharmacological activities, such as the potential antioxidant activity of scavenging oxygen radicals released by activating neutrophils[15], the Nrf2/HO-1 axis[16, 17], and the modulation of

[#] These authors contributed equally to this work.
[*] To whom correspondence should be addressed.
E-mail zhijianyangnj@njmu.edu.cn (Zhi-jian YANG);
jiyea@cpu.edu.cn (Ji-ye AA)
Received 2017-03-07 Accepted 2017-05-19

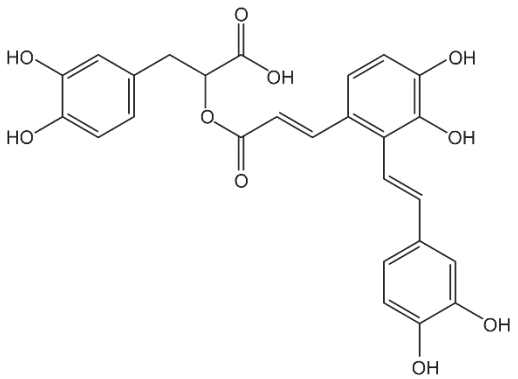


**Figure 1.** The chemical structure of salvianolic acid A.

NF-κB-dependent inflammatory pathways via IKKβ in RAW 264.7[18]. Several studies suggested that SAA can provide significant cardioprotection by inhibiting MMP-9 (matrix metalloproteinases-9) and its anti-apoptotic effects[19-21]. Moreover, SAA showed a protective effect by reducing cerebral ischemia/reperfusion injury[22, 23]. A previous *in vitro* study demonstrated that SAA provided full cerebral protection through the inhibition of granulocyte adherence by decreasing the expression of ICAM-1 (intercellular cell adhesion molecule-1) in brain microvascular endothelial cells[24]. Nevertheless, SAA, as a water-soluble phenolic acid, does not efficiently cross the blood brain barrier in sham rats. However, can SAA enter the central nervous system under conditions of increased permeability of the blood brain barrier induced by ischemia/reperfusion injury? Whether SAA has a role in metabolic regulation and protection in cerebral ischemia/reperfusion-induced damage is still unknown.

In the present study, metabolic patterns at the system level (*ie*, serum) and in local tissue (*ie*, brain tissue) were evaluated in model rats after ischemia/reperfusion and after treatment with SAA by employing a metabolomic platform based on GC-MS. Moreover, the distribution of SAA was examined in the brains of both sham and ischemia/reperfusion rats. We intended to explore the fundamental substances and the underlying mechanism that contribute to the efficacy of SAA in cerebral ischemia/reperfusion.

## Materials and methods

### Chemicals and reagents

SAA (purity 98%) was purchased from the Chengdu Must Biotechnology Co, Ltd (Chengdu, China). Vitamin C was purchased from Sinopharm Chemical Reagent Company Limited. [1,2-$^{13}C_2$] Myristic acid, the stable isotope-labeled internal standard (IS); methoxyamine hydrochloride (purity 98%); an alkane solution (C8–C40); and pyridine (99.8% GC) were purchased from Sigma-Aldrich. MSTFA (*N*-methyl-*N*-trimethylsilyl trifluoroacetamide) and 1% TMCS (trimethylchlorosilane) were obtained from the Pierce Chemical Company (Rockford, USA). ELISA kits for rat TNF-α, IL-1β, and IL-6 were purchased from Sigma-Aldrich (St Louis, USA). The test kits for the content of malondialdehyde (MDA) and the activity of superoxide dismutase (SOD) were purchased from the Nanjing Jiancheng Biology Research Institute (Nanjing, China). Methanol, acetonitrile and n-heptane were HPLC grade and obtained from Merck (Darmstadt, Germany). Purified water was produced by a Milli-Q system (Millipore, Bedford, USA).

### Animals

Male Sprague–Dawley (180–200 g) rats were purchased from B&K Universal Group Limited (Shanghai, China). The animals were cared for according to the Animal Facility Guidelines of the China Pharmaceutical University. All rats had free access to food and water under standard conditions (12/12 h light/dark cycle with a humidity of 65%±5%, 22–25 °C).

### Transient middle cerebral artery occlusion

tMCAO rats were prepared as previously described[25, 26]. The animals were anesthetized with 10% chloral hydrate (0.3 mL/100 g) by intra-peritoneal injection. A heating pad was used to maintain a rectal temperature of 37±0.3 °C during the experiment. After a median incision, the left carotid artery, external carotid artery, and internal carotid artery (ICA) were exposed. Branches of the external carotid artery were electrocauterized. Then, the ECA was ligated and cut approximately 3 mm above the bifurcation of the CCA, and a silk thread was tightened around the external carotid stump. A silicon-coated 4-0 monofilament nylon filament was inserted into the left ECA and advanced further into the ICA until a feeling of mild-resistance was achieved, indicating that the origin of the MCA was occluded. After the operation, the wound was sutured, and the animal recovered from anesthesia. Reperfusion was performed by releasing the nylon filament 2 h after the MCA occlusion.

### Pharmacokinetic study

Both sham-operated (sham) and model (I/R) rats received a dose of 10 mg/kg of SAA in the caudal vein, and rats in the I/R group received SAA when the reperfusion was performed. We collected whole blood and brain samples at 0.083, 0.5, 2, and 4 h. Whole blood was immediately centrifuged at 8000 revolutions per minute for 5 min to collect plasma and stored at -80 °C until analysis.

### Pharmacodynamics and metabolomics

After tMCAO, all rats were randomly divided into five groups: sham, which underwent the surgical procedure without suture insertion (Sham); 2 h MCAO followed by 0 h reperfusion (I); 6 h reperfusion (I/R-6 h); 12 h reperfusion (I/R-12 h); and 24 h reperfusion (I/R-24 h). The model rats received SAA (SAA-L: 5 mg/kg; SAA-H: 10 mg/kg) administration by intravenous injection or nimodipine (positive control, 1 mg/kg) by subcutaneous injection twice within 5 min when reperfusion was performed. We collected serum or brain samples for various analyses.

### Neurological deficit score and brain water content

A neurological test was performed on the rats by an examiner blinded to the experimental groups following a modified scoring system based on the one developed by Longa *et al*[25]

and Yang *et al*[27] as follows: 0, no deficits; 1, difficulty in fully extending the contralateral forelimb; 2, unable to extend the contralateral forelimb; 3, mild circling to the contralateral side; 4, severe circling; and 5, falling to the contralateral side.

The brain water content was determined using the standard wet-dry method[28]. The mice were euthanized under deep anesthesia at 24 h post-tMCAO, and the cerebrum was removed and placed on a prepared dry tray. Slices of approximately 2-mm thickness of the frontal pole and the cerebellum were removed. The slices were divided into ischemic and non-ischemic hemispheres. At the same time, the two hemisphere slices were packaged, respectively, with aluminum foil, their wet weights were evaluated with an electronic balance, and they were then dried for 24 h at 100 °C to determine the dry weights. The brain water content (BWC) was calculated as follows: BWC (%) = (wet weight − dry weight)/wet weight ×100.

### Brain infarct area

The infarct area of the brain was measured at 24 h after cerebral ischemia/reperfusion. The brains were dissected and placed in a refrigerator at 20 °C for approximately 15 min. Then, using a blade, the brain was cut into six 2-mm-thick slices and incubated in a 2% solution of 2,3,5-triphenyltetrazolium chloride (TTC) at 37 °C for 20 min in the dark. The slices were turned over to ensure that they were evenly dyed. With TTC staining, the sham tissue stained red and the infarct area remained pale. The TTC-stained slices were photographed and calculated using Image-ProPlus 5.1 software (Media Cybernetics, Inc, Bethesda, USA).

### Assay of inflammatory cytokines and MDA and the activity of SOD in brain tissue homogenate

At 6, 12, and 24 h of reperfusion after MCAO, the rats were euthanized under deep anesthesia. The brain tissue from the peri-infarct regions and the corresponding areas of sham-operated rats was homogenized in physiological saline (1:9, *w*/*v*). The supernatant and serum were collected and stored at −80 °C until use. The concentrations of TNF-α, IL-1β, IL-6, and MDA and the activity of SOD were detected using specific kits according to the manufacturers' instructions.

### Histopathological assessment by H&E and Nissl staining

Fresh rat brains were immediately immersed in 10% phosphate-buffered formalin for fixation and then implanted in paraffin. Five-micrometer-thick slices were cut from the coronal plane of the brain and stained with H&E and Nissl.

### Sample preparation and LC-MS/MS analysis

An aliquot of 50 μL of each plasma sample was pipetted into a 1.5-mL Eppendorf tube containing 10 μL of vitamin C, which was dissolved by 1 mol/L hydrochloric acid to improve the stability of SAA. Then, 50 μL of methanol containing the IS (5 μg/mL) was added and vortexed for 3 min to precipitate proteins. Extraction was carried out using 1 mL of ethyl acetate, followed by vortexing for 5 min. After centrifugation at 12 000×*g* for 5 min, a volume of 800 μL of the clear supernatant was transferred to a new Eppendorf tube. The extract liquor was evaporated to dryness. The residue was reconstituted in 100 μL of the mobile phase, and a 10-μL aliquot of supernatant was injected into the LC-MS/MS instrument for analysis. Brain tissue was homogenized in physiological saline (1:10, *w*/*v*). Then, 50 μL of brain homogenate was processed in accordance with the plasma.

The LC-MS/MS system consisted of a Shimadzu HPLC system 20A and an AB API4000 quadrupole mass spectrometer with an electrospray ionization (ESI) source. The HPLC separation was carried out on an Agilent Eclipse Plus C18 column (4.6 mm×150 mm, 5 μm, Agilent Technologies, USA). The chromatographic column was maintained at 40 °C. The mobile phase consisted of mobile phase A (0.2% formic acid in water) and mobile phase B (acetonitrile). The compounds were eluted in the following gradient conditions: the initial composition was 10% B, which was held for 0.2 min, then increased to 85% B in 3.8 min, and maintained for 1 min, followed by decreasing to 10% B within 1 min; the gradient was stopped at 9 min. The flow rate was 0.7 mL/min.

The eluate from the analytical column was introduced directly into the ESI source, which was operated in negative ion mode. The internal source voltage was 3.0 kV, and the endogenous temperature was maintained at 500 °C. Multiple reaction monitoring (MRM) was performed at *m*/*z* values of 493.3→295.2 for SAA and 321.0→152.0 for chloramphenicol. The IonSpray was set to 4500 V, and the collision energies of SAA and chloramphenicol were -70 eV and -60 eV, respectively.

### Sample preparation and GC–MS analysis

The same extraction, derivatization, and analysis procedures were applied as previously reported[29], with a few modifications. In brief, 200 μL of methanol containing 5 μg/mL of [1,2-$^{13}C_2$] myristic acid as an internal standard was added to 50 μL of serum or 20 mg of brain tissue to extract the metabolites and precipitate the protein. Then, 120 μL of supernatant was evaporated to dryness in a GC vial on an SPD2010-230 SpeedVac Concentrator (Thermo Savant, Holbrook, USA). Then, 30 μL of methoxyamine (10 mg/μL) in pyridine was added into the dried GC vial and vigorously vortexed for 3 min. Methoximation was carried out for 16 h at room temperature. Then, 30 μL of MSTFA was added with 1% TMCS as the catalyst for 1 h of trimethylsilylation. Finally, the solution was vortexed for 1 min after adding 30 μL of heptane with methyl myristate (30 μg/mL) as an external standard. The GC–MS analyses were performed as previously described[30]. Simply, the derivatized samples (0.5 μL) were injected onto a Shimadzu GCMS-QP2010 instrument (Shimadzu Corp, Tokyo, Japan) with an RTx-5MS (30 m×0.25 mm ID) fused-silica capillary column that was chemically bonded with a 0.25-μm cross bond of 5% diphenyl/95% dimethyl polysiloxane (Restek Corporation, PA, USA)[30]. Masses were scanned from 50 to 680 *m*/*z* at a rate of 30 spectra/s after a solvent delay of 270 s. The column temperature was initially maintained at 80 °C for 3 min and then increased to 300 °C at a rate of 20 °C/min, where it was held for 5 min. Automatic peak detection was

performed using Chroma TOF™ software (Leco, version 3.25) as previously reported[31]. The identification of endogenous metabolites was conducted by comparing the mass spectra and the retention indexes of the detected compounds with those of reference standards or those in available libraries such as the National Institute of Standards and Technology (NIST) library 2.0 (2008) and Wiley 9 (Wiley–VCH Verlag GmbH & Co KGaA, Weinheim, Germany).

### Data processing and analysis

The relative quantitative areas of each detected peak were normalized to an internal standard (IS). A partial least squares discriminant analysis (PLS-DA) and shared-and-unique-structures plots (SUS-plot) were carried out using SIMCA-P software (version 13.0, UMETRICS, Umeå, Sweden). The quality of the models was evaluated based on the relevant $R^2$ and $Q^2$ values.

### Statistical analysis

All values are expressed as the mean±SD. The statistical analyses consisted of one-way ANOVA, and $P<0.05$ was considered statistically significant.

## Results

### SAA regulated the neurological deficit and reduced the brain water content and the cerebral infarct area

The neurological deficit was examined and scored on a 6-point-scale at 24 h of reperfusion after tMCAO. Compared with the sham group, the model group showed, as expected, higher neurological deficit scores of 2.42±0.53, and the neurological deficit scores were significantly reduced to 1.57±0.53 and 1.14±0.69 in the SAA-L and SAA-H groups, respectively (Figure 2A). A significant increase was observed in the brain water content in the ischemic hemispheres in the model group up to 82.8%±0.75% (Figure 2B). The intravenous injection of SAA decreased the water content, indicating that SAA has a significant effect on the alleviation of cerebral edema. No infarction was observed in the sham group, but extensive lesions were found in both the striatum and the lateral cortex in the model group. The neuroprotective effects of SAA at different doses were evident, and the infarct size was significantly reduced in both the SAA-L and SAA-H groups compared with the sham group (Figure 2C and 2D).

### SAA decreased the level of inflammatory cytokines and MDA and enhanced the activity of SOD in the brain

The activity of SOD evidently decreased, and the content of MDA increased in the brain after cerebral ischemia following different times of reperfusion (6 h, 12 h and 24 h) (Figure 3A and 3B). Inflammatory cytokines, such as TNF-α and IL-1β, were stimulated (Figure 3C). The results indicate that the activity of SOD was elevated remarkably and that the

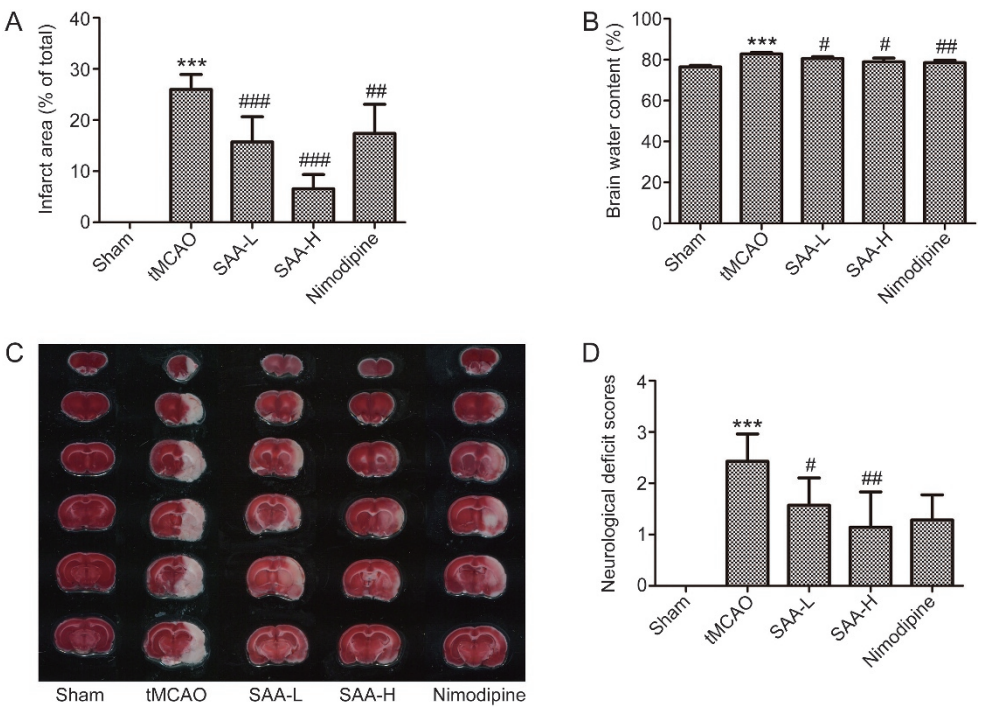


**Figure 2.** Effects of SAA on neurological deficit, infarct area and brain water content. (A) The neurological deficit scores of the rats (measured at 24 h of reperfusion after ischemia). Each value represents the mean±SD of independent experiments ($n$=7). (B) Brain water content ($n$=3). (C) Representative photographs of TTC staining of coronal brain sections (2-mm thickness) from rats (stained at 24 h of reperfusion after ischemia). The normal tissue stained red and the infarct area remained pale. (D) Infarct area. SAA-L (low dose, 5 mg/kg) and SAA-H (high dose, 10 mg/kg) were administered by intravenous injection when the reperfusion was performed. Each value represents the mean±SD of independent experiments ($n$=6–9). $^{***}P<0.001$, I/R-24 h *vs* sham; $^{\#}P<0.05$, $^{\#\#}P<0.01$, and $^{\#\#\#}P<0.001$, SAA *vs* I/R-24 h group.

concentrations of MDA, TNF-α and IL-1β in the brain tissue decreased after treatment with SAA.

### SAA alleviates the abnormal histopathology of brain tissue

Apparent interstitial edema was observed in the model group compared with the sham group, and the cellular morphology was abnormal, with swollen degeneration and shrunken nuclei (Figure 3D). In the SAA group, these abnormalities were significantly alleviated. The Nissl body is one of the characteristic structures of neurons, and SAA can noticeably increase the amount and the area of the Nissl body (Figure 3E). In combination with H&E staining, the results showed that SAA exerts a certain protection against cerebral injury caused by ischemia/reperfusion.

### Increased distribution of SAA in the brains of ischemia/reperfusion rats

The concentration of SAA in plasma gradually decreased with time in the sham group and in the I/R group (Figure 4A and 4D). However, the brain distribution of SAA in the model group slightly increased at 0.5 h, demonstrating more serious damage to the blood-brain barrier (Figure 4D and 4E). The concentration of SAA in the brains of model rats was significantly high compared to sham rats before 2 h after administration, especially at 0.5 h (up to 9.17 times). Good linearity of the kinetics of SAA was observed in the regression analysis of the plasma–brain concentration ($r^2$=0.999) in the sham rats (Figure 4C). In contrast, no linear correlation was observed between the concentrations in the plasma and the brain in the model rats (Figure 4F).

### Metabolic regulation of SAA in serum and brain tissue

Total ion chromatograms of serum and brain extracts are shown (Figure 5). We statistically calculated and identified 47 metabolites containing organic acids, amino acids, saccharides, and lipids that contribute the most to the model in

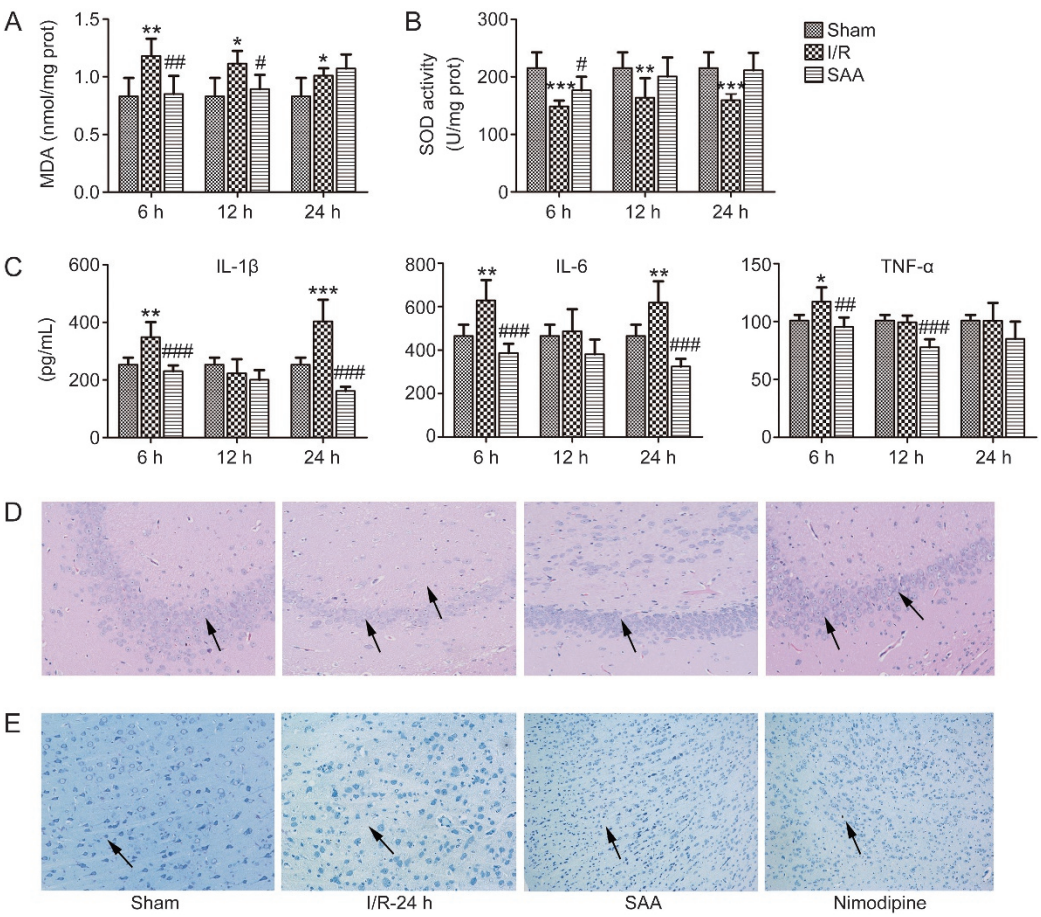


**Figure 3.** (A) The content of MDA in brain tissue homogenate (measured at 6, 12, 24 h of reperfusion after ischemia). Each value represents the mean±SD of independent experiments ($n$=5). (B) The activity of SOD in brain tissue homogenate (measured at 6, 12 and 24 h of reperfusion after ischemia). Each value represents the mean±SD of independent experiments ($n$=5). (C) The assessment of interleukin-1β (IL-1β), interleukin-6 (IL-6) and tumor necrosis factor-α (TNF-α) (measured at 6, 12 and 24 h of reperfusion after ischemia). Each value represents the mean±SD of independent experiments ($n$=6). Representative photographs of H&E (D) and Nissl (E) staining (stained at 24 h of reperfusion after ischemia) with a magnification of 200×. SAA (10 mg/kg) was administered by intravenous injection when the reperfusion was performed. $^{*}P$<0.05, $^{**}P$<0.01, and $^{***}P$<0.001, I/R *vs* Sham; $^{\#}P$<0.05, $^{\#\#}P$<0.01, and $^{\#\#\#}P$<0.001, SAA *vs* I/R.

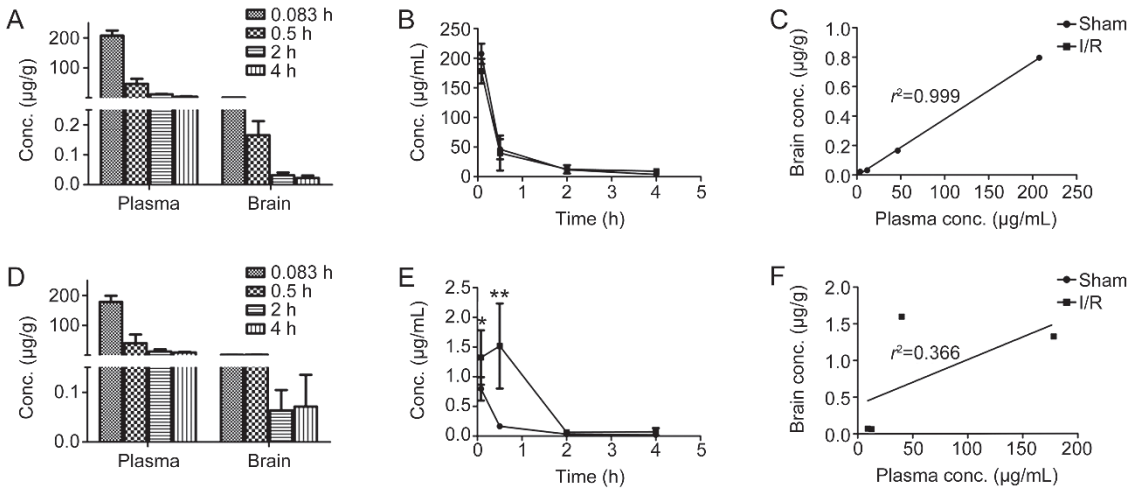


**Figure 4.** Brain distribution of SAA in the sham and I/R groups. The concentrations of SAA in the brains of the sham group (A) and the I/R group (D) at 0.083, 0.5, 2 and 4 h after treatment with SAA ($n$=3–7). The dynamic concentrations of SAA in the plasma (B) and the brain (E) between the sham and I/R rats. The linear correlativity between the SAA concentrations in the plasma and the brain in the rats of the sham group (C) and the I/R group (F). SAA (10 mg/kg) was administered by intravenous injection when the reperfusion was performed. $^{*}P<0.05$ and $^{**}P<0.01$, I/R *vs* Sham.

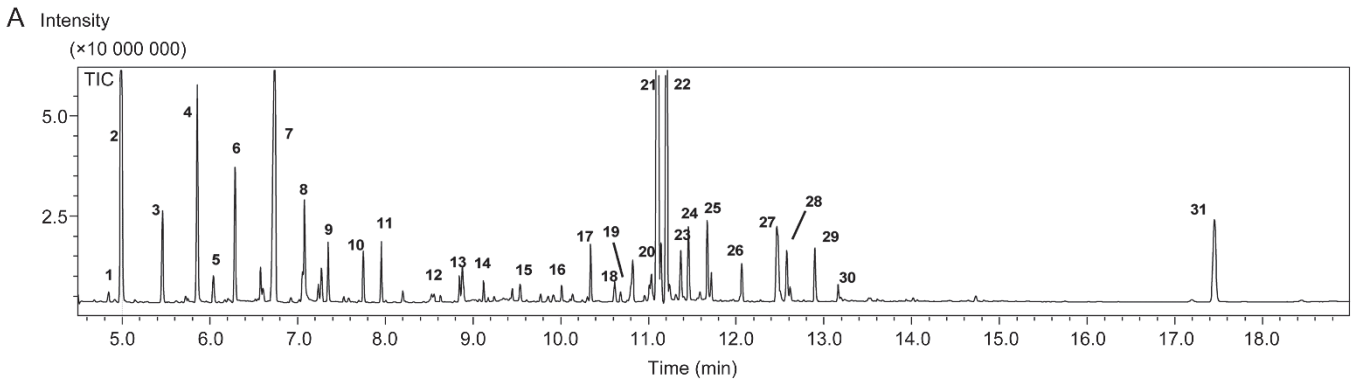


1. Pyruvic acid; 2. Lactate; 3. Alanine; 4. Oxalic acid; 5. 3-Hydroxybutyric acid; 6. Valine; 7. Urea; 8. Leucine;9. Glycine; 10. Serine; 11. Threonine; 12. Aspartic acid; 13. Malic acid; 14. Proline; 15. ES; 16. Glutamic acid; 17. Glutamine;18. Citric acid; 19. IS; 20. Lysine; 21. Glucose; 22. Tyrosine; 23. Inositol; 24. Maltose; 25. Palmitic acid; 26. Uric acid; 27. Oleic acid; 28. Tryptophan; 29. Glucuronic acid; 30. Arachidonic acid; 31. Cholesterol.

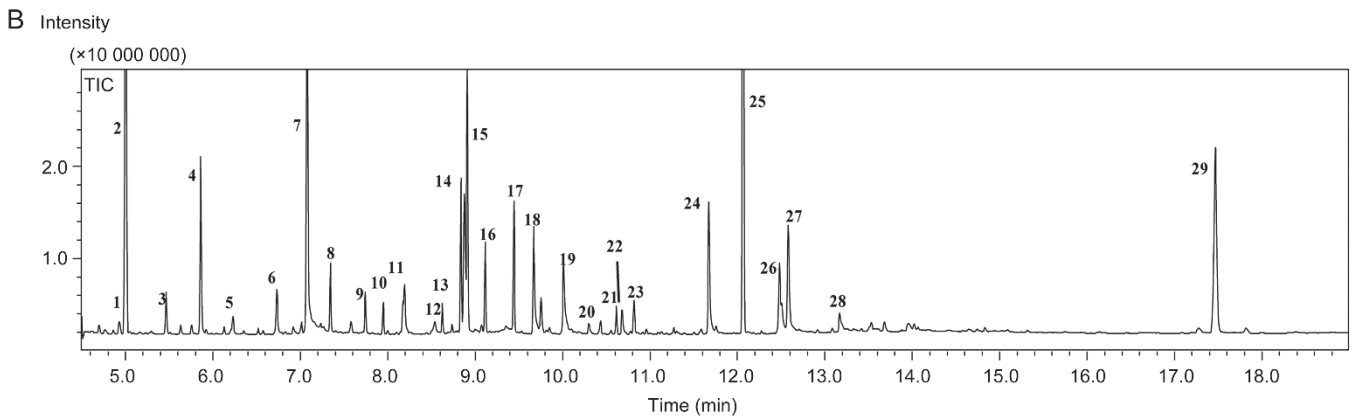


1. Pyruvic acid; 2. Lactate; 3. Alanine; 4. Oxalic acid; 5. U03; 6. Urea; 7. Leucine; 8. Glycine;9. Serine; 10. Threonine; 11. Aspartic acid; 12. Aminomalonic acid; 13. Malic acid; 14. Aspartic acid; 15. Proline; 16. Creatinine; 17. Glutamic acid; 18.N-Acetylaspartic acid; 19. ES; 21. Citric acid; 22. IS; 23. U06; 24. Palmitic acid; 25. Myo-Inositol; 26. Oleic acid; 27. Octadecanoic acid; 28. Arachidonic acid; 29. Cholesterol.

**Figure 5.** Total ion chromatograms (TICs) of serum (A) and brain (B) extracts and some identified compounds marked in the chromatograms.

serum ($P$<0.05) (Supplementary Table S1). The metabolism of the rats exhibited serious disorder after ischemia/reperfusion, and the administration of SAA slightly improved this outcome after 6 h of reperfusion; however, this was not significant after 24 h (Figure 6A and 6B). Fifty-one metabolites in the brain tissue were significantly different between the sham and the model groups (Supplementary Table S2). The metabolism of the brain tissue changed along with the reperfusion time, and different groups deviated to different extents (Figure 6D). The metabolic status of brain model group induced by two hours of ischemia followed by 24 h of reperfusion showed a marked shift compared with the sham group, but incubation with SAA deviated the anchoring of the model slightly compared with the sham controls, indicating a marginal regulatory effect on the metabolism (Figure 6E).

Orthogonal projections to latent structures (OPLS) is achieved by the comparison of two groups; therefore, shared-and-unique-structures plots (SUS-plots) were used for the comparison of three groups by the p (corr) values based on the two models of OPLS-DA[32]. The SUS plot showed an overall positive correlation between the variables in the two models of M24 versus S ($x$-axis) and M24 versus SAA24 ($y$-axis) (Figure 6C, 6F). The compounds that are of the same variation tendency in both the sham and the SAA groups compared with the model group cluster along the diagonal (red box). Compounds that changed only in the model group, but not in the SAA groups, are located along the $x$-axis (blue boxes; compounds that only contribute to the model). However, compounds that changed only in the SAA groups, but not in the model groups, are located along the $y$-axis (green boxes; compounds that only contribute to the SAA). We found that the compounds modulated by SAA were more abundant in the brain than in the serum (17 *vs* 4), which is consistent with the PLS-DA models that show lesser regulation by SAA in serum.

### SAA modulates the ischemia/reperfusion-induced perturbations of brain metabolites

Based on the discriminant metabolites identified in the brain tissue, the levels of lactate, TCA intermediates (fumaric acid, malic acid and citric acid), 5-HT, and amino acids (alanine, leucine, isoleucine and valine) increased, and the level of glutamic acid, glutamine and N-acetylaspartate gradually declined after reperfusion (Figure 7). Interestingly, the content of 3-hydroxybutyric acid increased in both serum and brain tissue, with a higher fold change in brain tissue (Figure 7F). The administration of SAA effectively modulated most of the metabolites toward normal metabolic homeostasis.

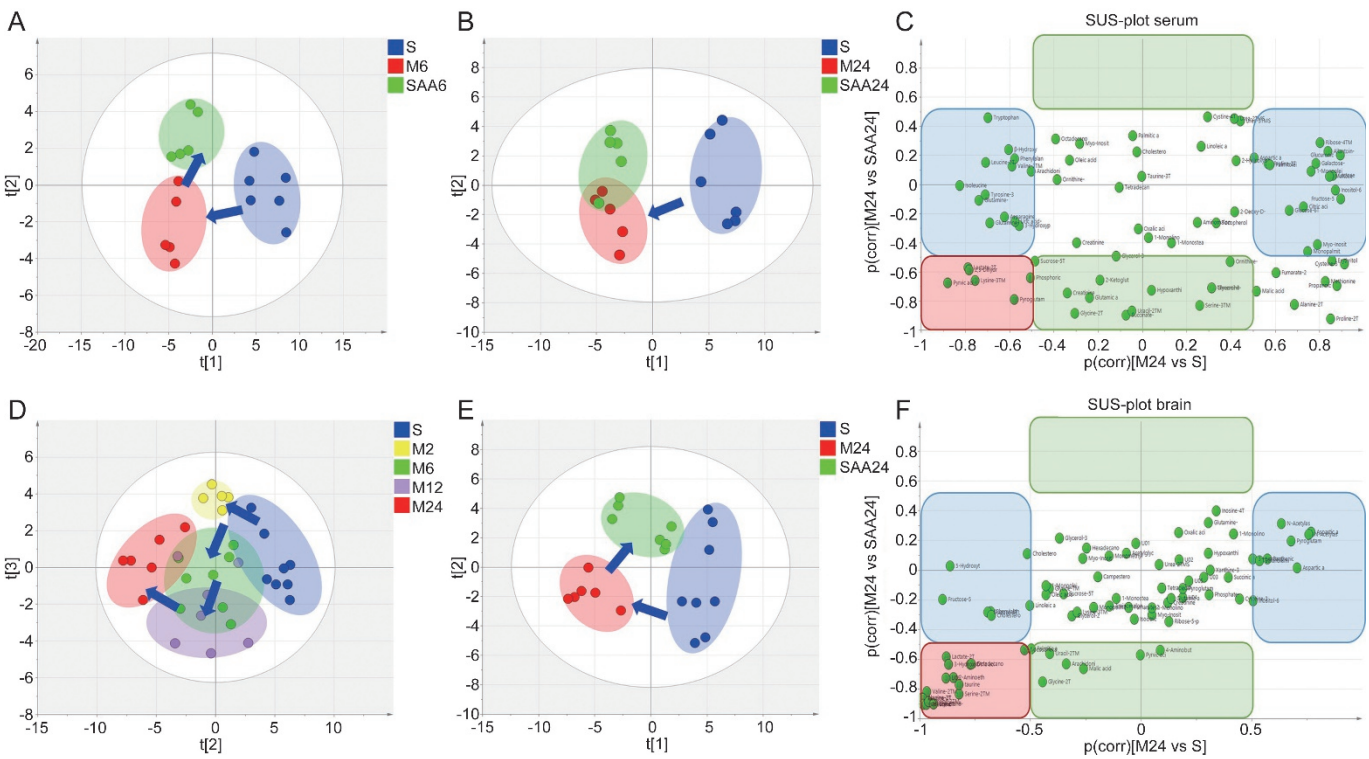


**Figure 6.** The partial least squares discriminant analysis (PLS-DA) of metabolites changes in serum (A, B) ($n$=5–6) and in brain tissue (D, E) ($n$=6–8) after ischemia/reperfusion injury. Shared and unique structure plot (SUS plot) of serum (C) and brain tissue (F) correlating the OPLS-DA models of M24 versus S ($x$-axis) and M24 versus SAA24 ($y$-axis). Accordingly, the variables in the lower left corners are the compounds that showed the reserved effect of SAA on ischemia/reperfusion injury (red box). However, metabolites located along the axes are specifically altered in the model group (blue boxes) and the SAA group (green boxes). S for Sham, M2 for I-2 h, M6 for I/R-6 h, M12 for I/R-12 h, M24 for I/R-24 h, SAA6 for I/R-6 h treated with SAA, and SAA24 for I/R-24 treated with SAA. SAA (10 mg/kg) was administered by intravenous injection when the reperfusion was performed.

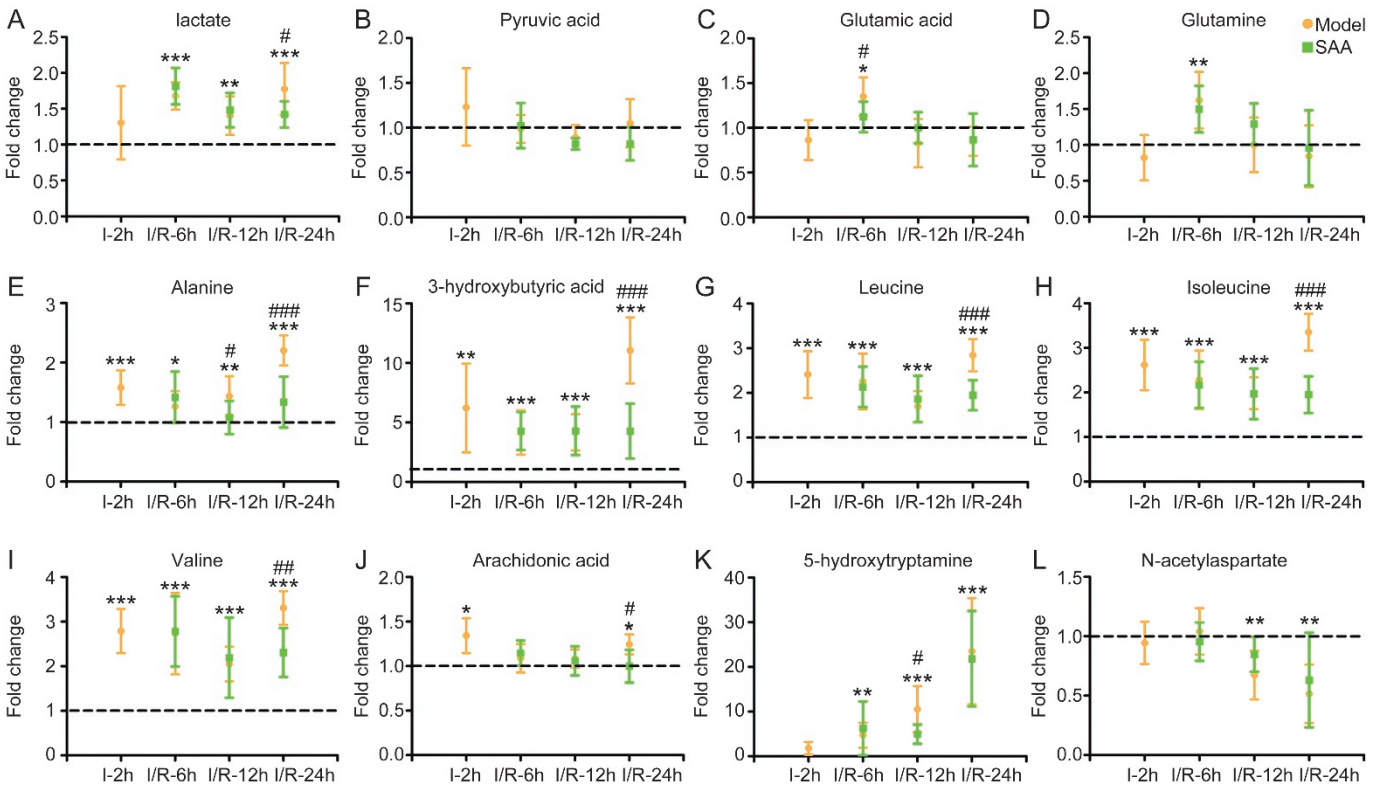


**Figure 7.** The representative metabolites changes compared to the sham group (dotted line) in the brain tissue during the ischemia/reperfusion time. SAA (10 mg/kg) was administered by intravenous injection when the reperfusion was performed. $^{*}P<0.05$, $^{**}P<0.01$, and $^{***}P<0.001$, Model *vs* Sham; $^{\#}P<0.05$, $^{\#\#}P<0.01$, and $^{\#\#\#}P<0.001$, SAA *vs* Model.

## Discussion

ROS can mediate a cascade of immune responses[33, 34], such as the stimulation of transcription factors, to directly induce significant pro-inflammatory cytokines production, including tumor necrosis factor-α (TNF-α), interleukin-1β (IL-1β), and interleukin-6 (IL-6)[35, 36]. Additionally, ROS and inflammatory cascades triggered by cerebral ischemic/reperfusion injury may further disrupt BBB integrity and amplify tissue damage[37, 38]. Previous reports have suggested that ischemia/reperfusion injuries can be alleviated with the use of antioxidant and anti-inflammatory agents[39]. SAA is a caffeic acid polymer that contains phenolic hydroxyls with a strong capacity for the scavenging of ROS. In the present study, our results clearly showed that SAA significantly decreased MDA levels and increased SOD. Pharmacologically, SAA showed consistent activities, such as a significant protection effect against cerebral ischemia/reperfusion injury, reductions in the cerebral infarct area and the brain water content, and improved neurological functions[40, 41]. Moreover, in this study, a GC/MS-based metabolomic platform was employed, and we examined the modulation effect of SAA on the perturbed metabolism of the brain and serum induced by ischemia/reperfusion. PLS-DA and the SUS-pot analysis showed better regulation of the metabolic pattern of brain than the serum with SAA, suggesting the positive effects of SAA on pathological brain tissue.

To address whether SAA exerts its pharmacological effect by targeting brain tissue directly after entering the central nervous system, for the first time, the pharmacokinetic properties of SAA were evaluated in the local brain tissue and the circulatory system in both ischemia/reperfusion model rats and sham rats. By comparing the data of the model and sham rats, we observed a markedly increased distribution of SAA in the brains of model rats compared to sham rats, and the level of SAA in the serum of model rats was not significantly different from the sham rats. It has been suggested that the disruption of the BBB induced by ischemia/reperfusion contributes to the increased level of SAA in the brains of model rats and the increased cerebral SAA facilitates the neuroprotective effect.

When large amounts of oxygen and nutritious substances were suddenly provided to cerebral ischemia tissue after reperfusion, oxidative stress and abnormalities of various functions of cerebral cells and cells that construct the BBB ensued[42]. For example, excessive oxygen resulted in an imbalance of reactive oxygen species in the mitochondrial respiratory chain, leading to cell death and protein degradation[43]. Moreover, our data showed significant elevations of lactate, TCA intermediates, branch chain amino acids, including leucine, isoleucine and valine, and 3-hydroxybutyric acid in the brain tissue, suggesting an increased supply and reduced utilization of the molecules. An injection of SAA efficiently reversed the perturbation of metabolism and the release of most of the molecules

induced by ischemia/reperfusion. The increased amount of SAA in the central nervous system may facilitate its direct protection and regulation of perturbed metabolism in a rat model of cerebral ischemia/reperfusion.

## Conclusions

SAA exhibited distinct protection against cerebral ischemia/reperfusion damage. SAA modulated the perturbed metabolism of serum induced by ischemia/reperfusion to a greater extent than that of the tissue, and the pharmacokinetic study revealed for the first time that the cerebral distribution of SAA in model rats is significantly higher than in sham rats. More SAA appeared to enter the central nervous system to facilitate its protective effect and regulation of the perturbed metabolism induced by cerebral ischemia/reperfusion in the model rats.

## Acknowledgements

This study was financially supported by the National Natural Science Foundation of China (81530098 and 81503342), the National Key Special Project of Science and Technology for Innovation Drugs of China (2015ZX09501001 and 2017ZX09301013), the Project for Jiangsu Province Key Lab of Drug Metabolism and Pharmacokinetics (BM2012012), and the Project of University Collaborative Innovation Center of Jiangsu Province (Modern Chinese Medicine Center and Biological Medicine Center).

## Author contribution

Ji-ye AA, Zhi-jian YANG and Guang-ji WANG designed this study; Si-qi FENG, Nan AA and Jian-liang GENG carried out the experiments; Jing-qiu HUANG, Run-bin SUN and Chun GE analyzed the data; Ji-ye AA, Si-qi FENG and Nan AA prepared the manuscript; Guang-ji WANG, Ji-ye AA and Lian-sheng WANG critically revised the manuscript. All authors have read and approved the final manuscript.

## Supplementary information

Supplementary information is available at the website of the Acta Pharmacologica Sinica.

## References

1 Siesjo BK. Mechanisms of ischemic brain damage. Crit Care Med 1988; 16: 954–63.
2 Di Carlo A. Human and economic burden of stroke. Age Ageing 2009; 38: 4–5.
3 Hacke W, Kaste M, Fieschi C, Von Kummer R, Davalos A, Meier D, *et al.* Randomised double-blind placebo-controlled trial of thrombolytic therapy with intravenous alteplase in acute ischaemic stroke (ECASS II). Second European-Australasian Acute Stroke Study Investigators. Lancet 1998; 352: 1245–51.
4 Marler JR, Tilley BC, Lu M, Brott TG, Lyden PC, Grotta JC, *et al.* Early stroke treatment associated with better outcome: the NINDS rt-PA stroke study. Neurology 2000; 55: 1649–55.
5 Allen CL, Bayraktutan U. Oxidative stress and its role in the pathogenesis of ischaemic stroke. Int J Stroke 2009; 4: 461–70.
6 Chen H, Yoshioka H, Kim GS, Jung JE, Okami N, Sakata H, *et al.* Oxidative stress in ischemic brain damage: mechanisms of cell death and potential molecular targets for neuroprotection. Antioxid Redox Signal 2011; 14: 1505–17.
7 Samson Y, Lapergue B, Hosseini H. Inflammation and ischaemic stroke: current status and future perspectives. Rev Neurol (Paris) 2005; 161: 1177–82.
8 Wang W, Dentler WL, Borchardt RT. VEGF increases BMEC monolayer permeability by affecting occludin expression and tight junction assembly. Am J Physiol Heart Circulat Physiol 2001; 280: H434–40.
9 Ho JH, Hong CY. Salvianolic acids: small compounds with multiple mechanisms for cardiovascular protection. J Biomed Sci 2011; 18: 30.
10 Katayama T, Nakashima H, Honda Y, Suzuki S, Yamamoto T, Iwasaki Y, *et al.* The relationship between acute phase serum amyloid A (SAA) protein concentrations and left ventricular systolic function in acute myocardial infarction patients treated with primary coronary angioplasty. Int Heart J 2007; 48: 45–55.
11 Jiang B, Li D, Deng Y, Teng F, Chen J, Xue S, *et al.* Salvianolic acid A, a novel matrix metalloproteinase-9 inhibitor, prevents cardiac remodeling in spontaneously hypertensive rats. PLoS One 2013; 8: e59621.
12 Fan HY, Fu FH, Yang MY, Xu H, Zhang AH, Liu K. Antiplatelet and antithrombotic activities of salvianolic acid A. Thromb Res 2010; 126: e17–22.
13 Xing JJ, Chen X, Tu PF, Jiang Y, Zhao JY. Effects of salvianolic acids on erythrocyte deformability in oleic acid induced acute lung injury in rabbits. Clin Hemorheol Microcirc 2006; 34: 507–17.
14 Wu ZM, Wen T, Tan YF, Liu Y, Ren F, Wu H. Effects of salvianolic acid A on oxidative stress and liver injury induced by carbon tetrachloride in rats. Basic Clin Pharmacol Toxicol 2007; 100: 115–20.
15 Lin TJ, Zhang KJ, Liu GT. Effects of salvianolic acid A on oxygen radicals released by rat neutrophils and on neutrophil function. Biochem Pharmacol 1996; 51: 1237–41.
16 Yang LL, Li DY, Zhang YB, Zhu MY, Chen D, Xu TD. Salvianolic acid A inhibits angiotensin II-induced proliferation of human umbilical vein endothelial cells by attenuating the production of ROS. Acta Pharmacol Sin 2012; 33: 41–8.
17 Zhang H, Liu YY, Jiang Q, Li KR, Zhao YX, Cao C, *et al.* Salvianolic acid A protects RPE cells against oxidative stress through activation of Nrf2/HO-1 signaling. Free Rad Biol Med 2014; 69: 219–28.
18 Oh KS, Oh BK, Mun JY, Seo HW, Lee BH. Salvianolic acid A suppress lipopolysaccharide-induced NF-kappa B signaling pathway by targeting IKK beta. Int Immunopharmacol 2011; 11: 1901–6.
19 Li YJ, Duan CL, Liu JX. Salvianolic acid A promotes the acceleration of neovascularization in the ischemic rat myocardium and the functions of endothelial progenitor cells. J Ethnopharmacol 2014; 151: 218–27.
20 Jiang BH, Li DF, Deng YP, Teng FK, Chen J, Xue S, *et al.* Salvianolic acid A, a novel matrix metalloproteinase-9 inhibitor, prevents cardiac remodeling in spontaneously hypertensive rats. PLoS One 2013; 8: e59621.
21 Xu TD, Wu X, Chen QP, Zhu SS, Liu Y, Pan DF, *et al.* The anti-apoptotic and cardioprotective effects of salvianolic acid A on rat cardiomyocytes following ischemia/reperfusion by DUSP-mediated regulation of the ERK1/2/JNK pathway. PLoS One 2014; 9: e102292.
22 Du G, Zhang J. Protective effects of salvianolic acid A against impairment of memory induced by cerebral ischemia-reperfusion in mice. Chin Med J (Engl) 1997; 110: 65–8.
23 Wang SB, Pang XB, Zhao Y, Wang YH, Zhang L, Yang XY, *et al.* Protection of salvianolic acid A on rat brain from ischemic damage via soluble epoxide hydrolase inhibition. J Asian Nat Prod Res 2012; 14:

1084–92.
24 Jiang M, Wang XY, Zhou WY, Li J, Wang J, Guo LP. Cerebral protection of salvianolic acid A by the inhibition of granulocyte adherence. Am J Chin Med 2011; 39: 111–20.
25 Longa EZ, Weinstein PR, Carlson S, Cummins R. Reversible middle cerebral artery occlusion without craniectomy in rats. Stroke 1989; 20: 84–91.
26 Lv P, Fang W, Geng X, Yang Q, Li Y, Sha L. Therapeutic neuroprotective effects of ginkgolide B on cortex and basal ganglia in a rat model of transient focal ischemia. Eur J Pharm Sci 2011; 44: 235–40.
27 Yang C, Zhang X, Fan H, Liu Y. Curcumin upregulates transcription factor Nrf2, HO-1 expression and protects rat brains against focal ischemia. Brain Res 2009; 1282: 133–41.
28 Mdzinarishvili A, Kiewert C, Kumar V, Hillert M, Klein J. Bilobalide prevents ischemia-induced edema formation *in vitro* and *in vivo*. Neuroscience 2007; 144: 217–22.
29 A J, Trygg J, Gullberg J, Johansson AI, Jonsson P, Antti H*, et al*. Extraction and GC/MS analysis of the human blood plasma metabolome. Anal Chem 2005; 77: 8086–94.
30 Zheng T, Liu LS, Shi J, Yu XY, Xiao WJ, Sun RB*, et al.* The metabolic impact of methamphetamine on the systemic metabolism of rats and potential markers of methamphetamine abuse. Mol Biosyst 2014; 10: 1968–77.
31 Jonsson P, Johansson AI, Gullberg J, Trygg J, A J, Grung B*, et al.* High-throughput data analysis for detecting and identifying differences between samples in GC/MS-based metabolomic analyses. Anal Chem 2005; 77: 5635–42.
32 Wiklund S, Johansson E, Sjostrom L, Mellerowicz EJ, Edlund U, Shockcor JP*, et al.* Visualization of GC/TOF-MS-based metabolomics data for identification of biochemically interesting compounds using OPLS class models. Anal Chem 2008; 80: 115–22.
33 Naik E, Dixit VM. Mitochondrial reactive oxygen species drive proinflammatory cytokine production. J Exp Med 2011; 208: 417–20.
34 Lakkur S, Judd S, Bostick RM, Mcclellan W, Flanders WD, Stevens VL*, et al.* Oxidative stress, inflammation, and markers of cardiovascular health. Atherosclerosis 2015; 243: 38–43.
35 Allan SM, Tyrrell PJ, Rothwell NJ. Interleukin-1 and neuronal injury. Nat Rev Immunol 2005; 5: 629–40.
36 Abulafia DP, De Rivero Vaccari JP, Lozano JD, Lotocki G, Keane RW, Dietrich WD. Inhibition of the inflammasome complex reduces the inflammatory response after thromboembolic stroke in mice. J Cereb Blood Flow Metab 2009; 29: 534–44.
37 Trendelenburg G. Molecular regulation of cell fate in cerebral ischemia: role of the inflammasome and connected pathways. J Cereb Blood Flow Metab 2014; 34: 1857–67.
38 Pun PB, Lu J, Moochhala S. Involvement of ROS in BBB dysfunction. Free Radic Res 2009; 43: 348–64.
39 Song J, Kang SM, Lee WT, Park KA, Lee KM, Lee JE. The beneficial effect of melatonin in brain endothelial cells against oxygen-glucose deprivation followed by reperfusion-induced injury. Oxid Med Cell Longev 2014; 2014: 639531.
40 Mahmood Q, Wang GF, Wu G, Wang H, Zhou CX, Yang HY*, et al*. Salvianolic acid A inhibits calpain activation and eNOS uncoupling during focal cerebral ischemia in mice. Phytomedicine 2017; 25: 8–14.
41 Wei LZ, Liu WP, Fei Z, Yi XC, Wang K, Luo Q*, et al.* Effects of salvianolic acid A on cerebral ischemia/reperfusion injury and antioxidase activities in rats. Prog Modern Biomed 2014.
42 Chen XM, Chen HS, Xu MJ, Shen JG. Targeting reactive nitrogen species: a promising therapeutic strategy for cerebral ischemia-reperfusion injury. Acta Pharmacol Sin 2013; 34: 67–77.
43 Jiang LM, Huang J, Wang YL, Tang HR. Metabonomic analysis reveals the $CCl_4$-induced systems alterations for multiple rat organs. J Proteome Res 2012; 11: 3848–59.